ChemComm

This article is part of the

Artificial photosynthesis
web themed issue

Guest editor: Andrew Benniston

All articles in this issue will be gathered together online at
www.rsc.org/photosynthesis

ChemComm

Dynamic Article Links

Cite this: *Chem. Commun.*, 2012, **48**, 1132–1134

www.rsc.org/chemcomm

COMMUNICATION

Electron transfer through α-peptides attached to vertically aligned carbon nanotube arrays: a mechanistic transition†‡

Jingxian Yu,[a] Ondrej Zvarec,[a] David M. Huang,[a] Mark A. Bissett,[b] Denis B. Scanlon,[a] Joe G. Shapter[b] and Andrew D. Abell*[a]

Received 27th October 2011, Accepted 1st December 2011
DOI: 10.1039/c2cc16665h

The mechanism of electron transfer in α-aminoisobutyric (Aib) homoligomers is defined by the extent of secondary structure, rather than just chain length. Helical structures (Aib units ≥ 3) undergo an electron hopping mechanism, while shorter disordered sequences (Aib units <3) undergo an electron superexchange mechanism.

The ability to transfer an electron from one biomolecule to another is critical to key biological processes, including photosynthesis and respiration.[1,2] This 'flow of electrons' is catalysed by oxidoreductases over surprisingly large molecular distances (>100 Å).[3,4] A number of factors influence the kinetics of this process, including peptide chain length, dipole orientation and hydrogen bonding.[5–9] Of particular significance is the suggestion that peptides can undergo electron transport *via* either a bridge-assisted superexchange or electron hopping mechanism, depending on the separation of electron donor and acceptor groups.[2,10–13] However, the exact role that these and other factors play in defining the mechanism is contentious.[10–12] In this paper, we present electrochemical evidence that the mechanism of electron transfer through oligomers of α-aminoisobutyric acids (Aib) is defined by secondary structure and associated intramolecular hydrogen bonding. Oligomers of Aib were used in the study since relatively short sequences (3 or more units) are known to form predictable and particularly stable helical structures.[14–16] The analysis was carried out by attaching the oligopeptides to vertically aligned single-walled carbon nanotube arrays/silicon electrodes (SWCNTs/Si, see Fig. 1a and the ESI‡) to provide a large surface area and rigid support for attachment, with excellent electron communication between electrodes and peptides.[17–22] SWCNTs/Si electrodes have previously been well characterised using a range of techniques,[21,23,24] and they are well documented for use in electrochemical studies.[20,21,25,26]

The required peptides were prepared by *N*-acylating ferrocenylmethylamine with oligomers of α-aminoisobutyric acid (see Fig. 1b and the ESI‡). The conformations of these were determined, by 2D-NMR spectroscopy, to be disordered and 3_{10}-helical for structures with n = 1–2 and n = 3–5 Aib units, respectively. This is consistent with related structures.[7,15] The prepared oligomers were separately attached to a SWCNTs/Si electrode prepared with an average nanotube separation (50 nm) significantly larger than the length of the peptides (see Table 1) in order to limit the possibility of electrochemical shortcuts (see the ESI‡). SWCNTs/Si functionalised with peptides containing 3, 4, and 5 Aib units gave IR absorptions at 1670 (amide I) and 1540 (amide II), which is consistent[4,27] with a 3_{10}-helical conformation on the surface (see the ESI‡). Electrochemical measurements of the immobilised oligopeptides (Fig. 1c) were then carried out in 0.1 M $TBAPF_6/CH_3CN$ solution using a specially designed electrochemical cell,[21] which provides a small working area (~0.2 mm^2) and tiny separation between working and reference electrodes. The ohmic-drop corrected electrochemical data were analysed as for other related studies.[13,28,29]

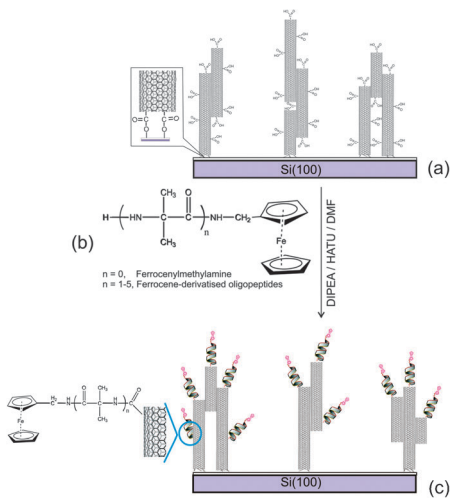

Fig. 1 Schematic of ferrocene-derivatised oligopeptide immobilised SWCNT array/silicon electrode and its fabrication.

[a] *School of Chemistry and Physics, The University of Adelaide, Adelaide, SA 5005, Australia. E-mail: andrew.abell@adelaide.edu.au; Fax: (+61) 8 8303 4358; Tel: (+61) 8 8303 5652*
[b] *School of Chemical & Physical Science, Flinders University, Bedford Park, SA 5042, Australia. E-mail: joe.shapter@flinders.edu.au; Fax: (+61) 8 8201 2905; Tel: (+61) 8 8303 2005*

† This article is part of the *ChemComm* 'Artificial photosynthesis' web themed issue.

‡ Electronic supplementary information (ESI) available: General information, synthesis of peptides, geometry of N-ferrocene-oligopetides, preparation of SWCNTs/Si arrays, attachment of ferrocene-oligopeptide to SWCNTs/Si arrays, characterisation of modified SWCNTs/Si arrays with attached ferrocene-oligopeptides, electrochemistry, discussions on the roles of SWCNT and Si surface in the electron transfer process. See DOI: 10.1039/c2cc16665h

Table 1 Electron transfer rate constants, apparent surface concentrations, formal potentials and iron-to-terminal nitrogen distances of ferrocenylmethylamine and ferrocene-derivatised oligopetides

Aib No.	Distance (Å)	Surface concentration ($\times 10^{-10}$ mole cm^{-2})	E_0 (V *vs.* SCE)	k_{app} (s^{-1})
0	4.36	4.86 ± 0.45	0.503	745.5 ± 56.4
1	5.37	7.91 ± 0.81	0.486	341.3 ± 29.1
2	6.39	6.22 ± 0.57	0.481	136.8 ± 16.3
3	9.93	2.04 ± 0.19	0.475	93.4 ± 9.2
4	12.30	4.68 ± 0.43	0.463	72.1 ± 5.6
5	14.12	2.15 ± 0.21	0.458	63.2 ± 4.3

A detailed calculation (see the ESI‡) on each sequential step in the overall electron transfer process in this system clearly shows that the electron transfer rate in the peptides is at least 8 orders of magnitude slower than that for all other electron transfer steps. Therefore we can safely ignore these other steps in the analysis of electrochemical data.

The resulting cyclic voltammograms show a pair of redox peaks with a significant non-faradaic background current (Fig. 2a). Well-formed redox peaks are observed at approx. 450 mV for the surface attached ferrocene-derivatised oligopeptide (Fig. 2b, n = 5, *i.e.* Aib$_5$-Fc) after background subtraction. The non-faradaic background current is attributed to capacitive effects associated with charging of the electrode/electrolyte interface[30] and was expected due to the rough surface.[25] The lack of a redox response from the control experiment (no coupling agents used for the preparation of control samples) excludes the possibility that the ferrocene-capped peptides are physically adsorbed.[20,25] The observed straight-line relationship between the oxidation/reduction currents and scan rate indicates that the electrode reaction occurs *via* a surface bound species.[31] This provides further evidence that the observed electrochemical redox peaks are due to the covalently anchored ferrocene-derivatised molecules. The FWHM (Full-Width Half-Maxima, Fig. 2b) for both the anodic and cathodic peaks are 160 and 150 mV respectively, greater than the theoretical value of 90.6 mV (ferrocene oxidation/reduction is a single electron process), indicating an inhomogeneous chemical environment of the Fc compounds on nanotubes.[32] Electrochemical data analysis using Laviron's methodology[33] (see the ESI‡) gave the electron transfer rate constants, surface concentrations, and formal potentials for ferrocenylmethylamine and the ferrocene-derivatised oligopeptides, as summarised in Table 1. The table also contains iron-to-terminal nitrogen distances for each structure, as determined by optimised geometries obtained using the hybrid B3LYP method with 6-31G** basis set (see the ESI‡).

The apparent surface concentrations (Table 1) are approx. 10 times greater than those obtained for peptides attached to flat gold electrodes.[27] This reflects the relative rough surface of the nanotube array, which accommodates the binding of a large amount of peptide.[22] This leads to improved reliability and reproducibility of the electrochemical response.[21] A graph (Fig. 3a) of electron transfer rate constant (k_{app}) *vs.* the iron-to-terminal nitrogen distance (as defined by the number of constituent monomers and secondary structure) reveals a clear dependence between the two parameters. A slope transition is observed on a change to structures containing more than two α-aminoisobutyric acid units (see the last 3 points on this graph). A similar transition has been demonstrated in DNA,[28] peptide nucleic acid[34] and polyproline-bridged systems.[13]

The structures that possess a well-defined helical conformation display a weak dependence of the electron transfer rate constant on distance, as evidenced by the shallow slope in Fig. 3a. This is consistent with a hopping mechanism.[11,13,28,35] The rate attenuation constant (β) was estimated to be 0.10 Å^{-1}. A plot of the inverse of the square root of k_{app} *vs.* the iron-to-terminal nitrogen distance (Fig. 3b) shows a straight line, which provides further evidence for a hopping mechanism.[4] The shorter sequences gave rise to a steep decrease, which is consistent with an alternative electron superexchange mechanism.[2,3,11,13] The apparent rate attenuation constant (β) for these peptides was calculated to be 0.84 Å^{-1}. These rate attenuation constants are smaller than those reported for an oligoproline-bridge

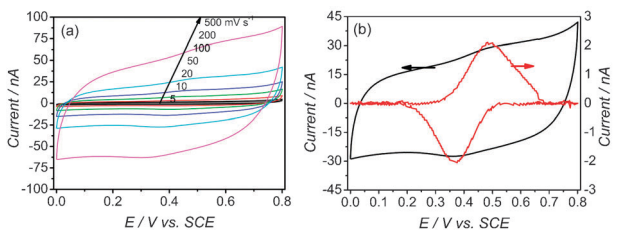

Fig. 2 (a) Cyclic voltammograms of ferrocene-derivatised oligopeptide (n = 5) modified SWCNTs/Si electrode in 0.1 mol L^{-1} TBAPF$_6$/CH$_3$CN solution, with the scan rate v of 5, 10, 20, 50, 100, 200 and 500 mV s^{-1} from the centre to upright. (b) Baseline subtracted cyclic voltammogram at 200 mV s^{-1}.

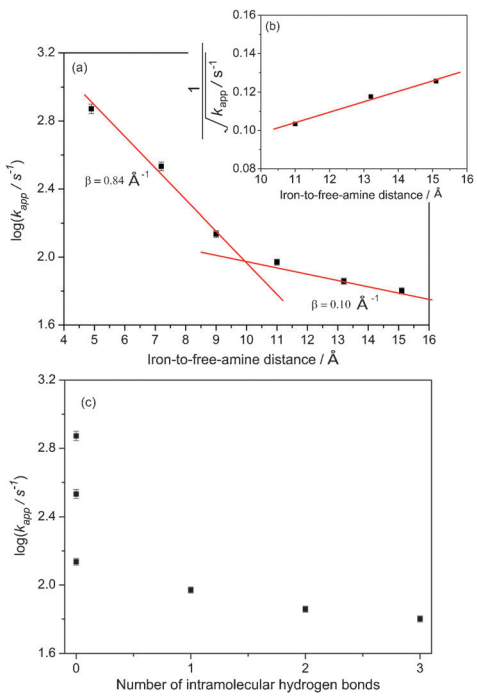

Fig. 3 (a) Dependence of k_{app} on iron-to-terminal nitrogen distance. (b) Plot of the inverse of the square root of k_{app} *vs.* the iron-to-terminal nitrogen distance for the helical peptides (n = 3–5). (c) Dependence of k_{app} on the number of intramolecular hydrogen bonds. (Data points from top to bottom and left to right in (a) and (c) represent derivatives with increasing number of Aib units).

diruthenium structure that also shows a slope transition and hence two constants.[13] We believe this difference to be attributable to a combination of the donor, bridge and acceptor.[1,36]

The structures giving rise to the first three points in Fig. 3a adopt a disordered conformation and hence lack defined intramolecular hydrogen bonding. Here the electron transfer rate constant is clearly dependent on the number of Aib units and hence the iron-to-terminal nitrogen distance. By comparison, the three helical structures (represented by the last three points in Fig. 3a) possess well-defined intramolecular hydrogen bonding (1, 2, and 3 bonds respectively[7,15]) that defines their secondary helical structure and hence the iron-to-terminal nitrogen distance and mechanism of electron transfer. This dependence of k_{app} on the number of intramolecular hydrogen bonds is depicted in Fig. 3c. The electron transfer rate constant depends strongly on intramolecular hydrogen bonding, which facilitates the observed electron hopping mechanism. This is consistent with theoretical studies,[37] and experimental work that reveals that an increase in the number of intramolecular hydrogen bonds results in better donor/acceptor electronic coupling.

A previous study on oligopeptides reports a significant decrease in k_{app} on increasing the number of intramolecular hydrogen bonds from zero to one,[7] with a much reduced decrease for larger sequences containing further intramolecular hydrogen bonding. The same phenomenon is observed in Fig. 3c. However electron transfer was reported to occur *via* an electron superexchange mechanism in the previous study.[7] We suggest that these data are consistent with a transition from superexchange to a hopping mechanism, due to a change from a disordered to a well-defined helical conformation. Furthermore, our results suggest a reinterpretation of the observed weak dependence[12] between the k_{app} and number of intramolecular hydrogen bonds for helical oligopeptides in solution containing *p*-cyanobenzamide donor and tertbutylperoxide acceptor groups. Our work indicates an electron transfer hopping mechanism with participation from the constituent intramolecular hydrogen bonds, rather than the previously reported electron transfer superexchange mechanism.

In conclusion, electrochemical studies are reported on oligomers of Aib attached to a single-walled carbon nanotube array/p-silicon (100) electrode to begin to unravel factors influencing the mechanism of electron transfer. Our data suggests that electron transfer in helical structures occurs by a hopping mechanism, with the amide bonds providing hopping sites, and facilitation from intramolecular hydrogen bonds. Shorter conformationally disordered sequences undergo electron transfer *via* an alternative electron superexchange mechanism. A mechanistic transition is apparent on increasing the number of Aib units from 2 to 3.

The work was financially supported by the Australian Research Council (DP0985176).

Notes and references

1 S. S. Isied, M. Y. Ogawa and J. F. Wishart, *Chem. Rev.*, 1992, **92**, 381.
2 M. Cordes and B. Giese, *Chem. Soc. Rev.*, 2009, **38**, 892.
3 T. R. Prytkova, I. V. Kurnikov and D. N. Beratan, *Science*, 2007, **315**, 622.
4 Y. Arikuma, H. Nakayama, T. Morita and S. Kimura, *Angew. Chem., Int. Ed.*, 2010, **49**, 1800.
5 P. A. Brooksby, K. H. Anderson, A. J. Downard and A. D. Abell, *Langmuir*, 2010, **26**, 1334.
6 B. R. Chaudhry, J. Wilton-Ely, A. B. Tabor and D. J. Caruana, *Phys. Chem. Chem. Phys.*, 2010, **12**, 9996.
7 S. Antonello, F. Formaggio, A. Moretto, C. Toniolo and F. Maran, *J. Am. Chem. Soc.*, 2003, **125**, 2874.
8 D. N. Beratan, J. N. Betts and J. N. Onuchic, *Science*, 1991, **252**, 1285.
9 E. Galoppini and M. A. Fox, *J. Am. Chem. Soc.*, 1996, **118**, 2299.
10 J. Watanabe, T. Morita and S. Kimura, *J. Phys. Chem. B*, 2005, **109**, 14416.
11 Y. T. Long, E. Abu-Rhayem and H. B. Kraatz, *Chem.–Eur. J.*, 2005, **11**, 5186.
12 F. Polo, S. Antonello, F. Formaggio, C. Toniolo and F. Maran, *J. Am. Chem. Soc.*, 2005, **127**, 492.
13 R. A. Malak, Z. N. Gao, J. F. Wishart and S. S. Isied, *J. Am. Chem. Soc.*, 2004, **126**, 13888.
14 O. Jacobsen, H. Maekawa, N. H. Ge, C. H. Gorbitz, P. Rongved, O. P. Ottersen, M. Amiry-Moghaddam and J. Klaveness, *J. Org. Chem.*, 2011, **76**, 1228.
15 A. Donoli, V. Marcuzzo, A. Moretto, C. Toniolo, R. Cardena, A. Bisello and S. Santi, *Org. Lett.*, 2011, **13**, 1282.
16 D. F. Kennedy, M. Crisma, C. Toniolo and D. Chapman, *Biochemistry*, 1991, **30**, 6541.
17 P. Diao and Z. F. Liu, *Adv. Mater.*, 2010, **22**, 1430.
18 K. T. Constantopoulos, C. J. Shearer, A. V. Ellis, N. H. Voelcker and J. C. Shapter, *Adv. Mater.*, 2010, **22**, 557.
19 O. A. de Fuentes, T. Ferri, M. Frasconi, V. Paolini and R. Santucci, *Angew. Chem., Int. Ed.*, 2011, **50**, 3457.
20 J. X. Yu, S. Mathew, B. S. Flavel, M. R. Johnston and J. G. Shapter, *J. Am. Chem. Soc.*, 2008, **130**, 8788.
21 J. X. Yu, J. G. Shapter, J. S. Quinton, M. R. Johnston and D. A. Beattie, *Phys. Chem. Chem. Phys.*, 2007, **9**, 510.
22 J. J. Gooding, R. Wibowo, J. Q. Liu, W. R. Yang, D. Losic, S. Orbons, F. J. Mearns, J. G. Shapter and D. B. Hibbert, *J. Am. Chem. Soc.*, 2003, **125**, 9006–9007.
23 J. X. Yu, D. Losic, M. Marshall, T. Bocking, J. J. Gooding and J. G. Shapter, *Soft Matter*, 2006, **2**, 1081.
24 C. J. Shearer, J. Yu, K. M. O'Donnell, L. Thomsen, P. C. Dastoor, J. S. Quinton and J. G. Shapter, *J. Mater. Chem.*, 2008, **18**, 5753.
25 J. X. Yu, J. G. Shapter, M. R. Johnston and J. S. Quinton, *Electrochim. Acta*, 2007, **52**, 6206.
26 B. S. Flavel, J. Yu, J. G. Shapter and J. S. Quinton, *Electrochim. Acta*, 2008, **53**, 5653.
27 S. Okamoto, T. Morita and S. Kimura, *Langmuir*, 2009, **25**, 3297.
28 B. Giese, J. Amaudrut, A. K. Kohler, M. Spormann and S. Wessely, *Nature*, 2001, **412**, 318.
29 D. H. Waldeck and D. E. Khoshtariya, *Mod. Aspects Electrochem.*, 2011, **52**, 105.
30 P. Bertoncello, J. P. Edgeworth, J. V. Macpherson and P. R. Unwin, *J. Am. Chem. Soc.*, 2007, **129**, 10982.
31 A. J. Bard and L. R. Faulkner, *Electrochemical Methods: Fundamentals and Applications*, 2nd edn, Wiley, New York, 2000.
32 J. Q. Liu, A. Chou, W. Rahmat, M. N. Paddon-Row and J. J. Gooding, *Electroanalysis*, 2005, **17**, 38.
33 E. Laviron, *J. Electroanal. Chem.*, 1979, **100**, 263.
34 A. Paul, R. M. Watson, E. Wierzbinski, K. L. Davis, A. Sha, C. Achim and D. H. Waldeck, *J. Phys. Chem. B*, 2010, **114**, 14140.
35 Q. Lu, K. Liu, H. M. Zhang, Z. B. Du, X. H. Wang and F. S. Wang, *ACS Nano*, 2009, **3**, 3861.
36 O. S. Wenger, *Acc. Chem. Res.*, 2011, **44**, 25.
37 J. Yu, D. M. Huang, O. Zvarec, J. G. Shapter and A. D. Abell, 2011, in preparation.

